IEEE Access
Multidisciplinary | Rapid Review | Open Access Journal

Received April 23, 2020, accepted July 12, 2020, date of publication July 31, 2020, date of current version August 20, 2020.

Digital Object Identifier 10.1109/ACCESS.2020.3013298

The propagation of the Ion-Flow Near the AC Transmission Lines

YI TIAN[1,2], CHIFENG LIU[1], XINBO HUANG[1,3], (Senior Member, IEEE), WENCHAO TIAN[3], WEN CAO[1], YONGCAN ZHU[1], AND LONG ZHAO[1]

[1]Department of Electronics and Information, Xi'an Polytechnic University, Xi'an 710048, China
[2]Department of Electrical Engineering, Xi'an Jiaotong University, Xi'an 710048, China
[3]Department of Electrical and Mechanical Engineering, Xidian University, Xi'an 710071, China

Corresponding author: Xinbo Huang (huangxb1975@ 163.com)

This work was supported in part by the China Postdoctoral Science Foundation under Grant 2019M653631, in part by the Key Research and Development plan of Shaanxi under Grant 2020ZDLGY09-10, and in part by the Natural Science Basic Research Program of Shaanxi under Grant 2018JM513.

ABSTRACT The series of physical processes contained in the corona layer is the source of space ions formed by the corona discharge of the high-voltage AC line. However, since these physical processes are difficult to calculate accurately and the corona layer thickness is usually small, the corona layer is ignored in the published literature on the corona discharge of the AC line, and the ions are considered to be emitted directly from the conductor surface. In this paper, the distribution area of the charged particles is divided into the corona plasma region and the unipolar drift region. A mathematical physical model of the photoionization and photoemission, which sustain self-sustaining discharge in the positive and negative half-cycle of corona plasma region of the AC conductor in dry air, are established. The influence of the ions generated in the previous cycle is also considered in the numerical simulation process. Finally, a complete microscopic physical model describing the corona discharge of the AC conductor under dry air is established. The validity of the physical model proposed in this paper is demonstrated by comparison with experimental results reported in the literature. Through the numerical simulation of the ion flow field of positive and negative half-cycle and the corona current, the physical process of the corona discharge around the AC line is better understood and analysed. Further positive and negative half-cycle charged particle motion and corona plasma regions were compared and analyzed. This work provides a brand new mathematical physics method for understanding and applying AC corona discharge.

INDEX TERMS Corona discharge, high-voltage AC line, microscopic physical process, photoionization, photoemission.

I. INTRODUCTION

High-voltage AC transmission lines have been widely used to meet the growing electricity demand of society. When the electric field near the high-voltage conductor exceeds the onset field strength, the corona discharge occurs around the conductor [1]. Corona is a partial breakdown of the gas in the electric field and involves many complex phenomena, including the generation of the excited molecule state of the space charge and its components [2]. The dry air is mainly composed of nitrogen and oxygen, both of which have a wide range of excited states [3]. Oxygen itself is additionally an electronegative gas and has the ability to attach electrons [4]. These phenomena are combined to influence the generation of electric field and secondary electrons, thereby giving corona its unique pattern. This work provides an invaluable guideline for a better understanding of the microphysical process and industrial applications of AC corona discharge [5]–[8].

A series of physical processes such as impact ionization, electron attachment, and secondary electron emission included in the corona plasma layer is the source of the formation of space ions in the corona discharge of the high-voltage AC line [9]. However, it is difficult to establish mathematical models to accurately describe these physical processes. These physical processes are usually overlooked when studying AC corona discharge. When the AC voltage is applied to the conductor, the ion moves a very short distance away from

The associate editor coordinating the review of this manuscript and approving it for publication was Lei Wang.

the conductor, and then returns to the latter, and afterward moves back and forth alternately. The total decrease in the potential of the ions in this displacement depends on the displacement law. The potential drop has the same order of magnitude as the line voltage, which means that the ionization energy is completely insignificant compared to the energy consumed by the charge during the charge displacement process. The experiments in the literature are basically based on the test research of corona parameters such as the onset field and the current in the external circuit. However, since the duration of microscopic physical process of corona discharge in the corona plasma layer is extremely short (nanosecond) [10], [11], as well as unpredictable propagation paths and low radiation from the streamer, it is difficult to obtain microscopic discharge parameters (ion current density, charge distribution, electric field in the corona layer) by experimental testing. With the continuous development and optimization of spatial discrete methods, the theoretical research based on numerical simulation of discharge development has been carried out [12]–[17]. To facilitate numerical simulation, most of these studies are based on the hydrodynamic convection-diffusion model to describe the distribution and development of plasma. Corona is a self-sustaining discharge in the positive and negative periods of the AC voltage, which is maintained self-sustaining discharge through secondary processes. The secondary processes include photoemission from the discharge electrode, bombardment of the discharge surface by the positive ions, or photoionization in the gas [2], [8]. The secondary process is a challenge for many numerical studies [18], [19], and the effect of precision on the numerical algorithm is imposed by applying constraints. For a secondary process, the balance between computational efficiency and precision are a high computationally demanding problem, but appropriate modeling of the discharge and breakdown phenomena is still critical. Therefore, there is a need to develop programs that accurately and effectively capture the nature of these physical processes. A simple approximation for the secondary process of the model, such as constant background ionization [12], one-dimensional photoionization model [20], equivalent ion-impact, is incorporated into a two-dimensional solution. With the continuous development of finite element method, the numerical simulation efficiency has been greatly improved. Therefore, the full modeling of the secondary phenomena can be carried out by numerical study of various parameters, thus giving an insight into the deeper physical processes.

In this paper, the microscopic physics processes of the corona discharge near the AC conductor in dry air, where the distribution region of charged particles is divided into corona plasma layer and unipolar region, is analyzed numerically through a two-dimensional numerical model. Depending on the onset field strength of the positive and negative half-cycle, an AC voltage cycle is divided into six stages to study the microscopic movement of the charged particles of the corona discharge. In the positive and negative half-cycles of the voltage, the secondary processes of self-sustaining discharge are mainly photoionization and photoemission. The two-dimensional numerical models are used to establish and study the physical model and the mechanism of the secondary process. The corona current of AC conductor is predicted, which is in accordance with the experimental test reported in the literature. The ion distribution of the positive and negative half-cycles is numerically analyzed. The aim is to further investigate the microscopic physical processes of the plasma motion near the surface of the AC conductor.

II. MODEL FORMULATION

A. PHYSICAL DESCRIPTION

On AC transmission lines, the conductor voltage is periodically variable and there are a lot of positive and negative ions around the conductor. Consequently, AC corona discharge is no longer a simple alternation of positive and negative corona discharge and is different from what would be expected if the positive and negative DC lines were operating independently. In addition, the onset field of the positive and negative half-cycle is influenced by the ions generated by the last half-cycle, as shown in Figure 1, so that discharge onset is not satisfied by Peek's onset field but needs to be amended.

Before point A, corona discharge does not occur on the conductor because the corona voltage is not reached; when the conductor potential reaches at point A, the conductor starts corona discharge. From this point on, the electron avalanche will develop to conductor surface with the increasing of electric field. Thus, the ionization activity of the highest enhanced electric field occurs on the conductor surface (see Figure 2(a)).

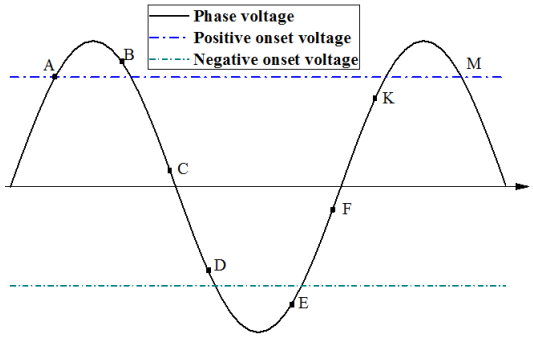

FIGURE 1. Transformation of the onset filed in the corona discharge sequence.

Photoionization which sustains self-sustained discharge is the main source of the secondary electron for a positive corona discharge. Due to the presence of a large number of positive ions around the conductor, the conductor potential (point B) that stops the positive corona is higher than the corona onset. The termination of corona discharge will stop the generation of positive ions, whereas the positive ions generated by discharge continue to move outward. When the conductor potential reaches point C, the electric field around the conductor begins to reverse. The negative corona discharge begins at point D due to the presence of a large number of positive ions around the conductor; subsequently,

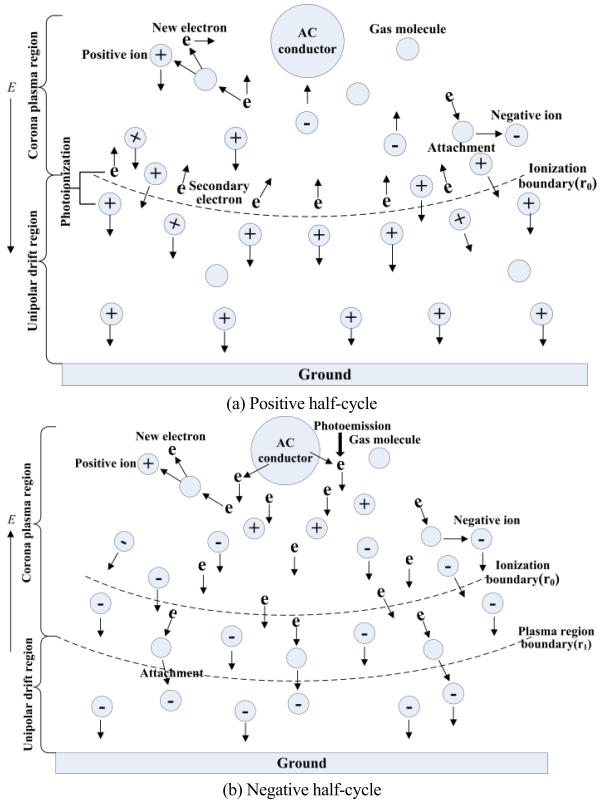

FIGURE 2. The physical process AC corona discharge.

the regular interval of the discharge pulse is generated, that is, Trichel pulse, while the pulse frequency will increases with the applied voltage increases. Eventually, a stable glow discharge is formed at a higher voltage level (see Figure 2(b)).

The main secondary process for the negative corona discharge is the photoemission at the negative conductor surface. Electrons from the ionization layer rapidly enter the surrounding air, and negative ions are formed through adsorption of neutral air molecules and particles in the plasma layer. After that, the recombination between these negative ions and positive ions generated by positive corona discharge and impact ionization occurs in negative corona discharge. After the conductor potential develops to point E, the corona discharge will terminate and negative ions will not be formed, but negative ions and electrons will continue to move towards the outside. After the conductor potential reaches point F, the electric field around the conductor begins to change from negative to positive. The conductor potential increases quickly to point K, at which point a positive discharge corona is started even through the applied voltage is below the onset level because the presence of a large number of negative ions around the conductor enhances the conductor field. The process is now repeated from cycle to cycle.

Each AC cycle is divided into n time segments Δt. At the ith time step, the instantaneous applied voltage on the conductor is expressed as:

$$U_{app} = U_{\max} \sin\left[\omega(i-1)\Delta t\right] \tag{1}$$

where $U_{\max}$ is the maximum AC voltage; ω is angular frequency.

The onset field can be derived from Peek'formula (equation (3)) and equation (4) [16]. The presence of large amounts of ions (which include the opposite ions produced by the last half-cycle, identical ions and electrons produced in this cycle) around the conductor modify the local field. The identical ions are dominated in the corona by the later analysis. Therefore, the electric field E_i generated by these opposite without corona discharge and identical ions in the corona on the surface of the conductor is taken into account in this paper. These changes the onset field E_{ci}, and hence the corrected onset field becomes as follows:

$$E_{ci} = E_c \mp E_i \tag{2}$$

where

$$E_c = E_{\mathrm{m}}\delta m\left(1 + \frac{K}{\sqrt{\delta r}}\right)\left(\frac{\mathrm{kV}}{\mathrm{cm}}\right) \tag{3}$$

here E_{m} is the empirical constant, $E_{\mathrm{m}} = 30.3\mathrm{kV/cm}$; δ is the relative air density; m is the roughness factor of conductor surface, between 0.3 and 0.8; r is the conductor radius; K is the empirical constant, $K = 0.298$.

$$E_i = \int_{\Omega} \frac{\rho\vec{r}}{4\pi\varepsilon_0 r^3} ds = \int_{\Omega} \frac{\rho cos\theta}{4\pi\varepsilon_0 r^2} ds \tag{4}$$

here ρ is the ions density; θ is the angle between electric field direction generated by ions on the conductor surface and the normal vector, and ε_0 is the permittivity of free space; r is the distance between conductor surface and ions; Ω is a bounded convex polygonal domain in R^2.

B. GOVERNING EQUATIONS

According to the above description of the corona discharge model of AC conductor, the corona discharge of AC conductor includes two kinds of discharge processes: the positive and negative corona discharge as its voltage cycle changes. Based on the hydrodynamics convective-diffusion model, two kinds of corona discharge models include the electron, positive and negative ion convection-diffusion equations coupled with Poisson's equation:

$$\nabla^2 u = -\frac{(N_p - N_e - N_n)e}{\varepsilon_0} \tag{5}$$

$$\begin{aligned}\frac{\partial N_e}{\partial t} &= -\nabla\cdot(N_e k_e \boldsymbol{E} - D_e\nabla N_e) + \alpha N_e\left|k_e\boldsymbol{E}\right| \\ &\quad - \eta N_e\left|k_e\boldsymbol{E}\right| - \beta_{ep}N_e N_p + S_{ph}\end{aligned} \tag{6}$$

$$\begin{aligned}\frac{\partial N_p}{\partial t} &= -\nabla\cdot(N_p k_p \boldsymbol{E}) + \alpha N_e\left|k_e\boldsymbol{E}\right| \\ &\quad - \beta_{ep}N_e N_p - \beta_{np}N_n N_p + S_{ph}\end{aligned} \tag{7}$$

$$\frac{\partial N_n}{\partial t} = -\nabla\cdot(N_n k_n \boldsymbol{E}) + \eta N_e\left|k_e\boldsymbol{E}\right| - \beta_{np}N_n N_p \tag{8}$$

where u is the electric potential; N_e, N_n, N_p are the electron, negative and positive ion densities; k_e, k_n, k_p are the electron, negative and positive ion mobility; e is the electronic charge. The symbols α, η, β and D denote the ionization,

attachment, recombination and electron diffusion coefficient, respectively. The air transport parameters here can be represented by the equations, as described by Morrow and Lowke [16], [17], [21], [22]. The term S_{ph} is the rate of ion-electron pair generated by the photoionization.

Continuity Equations (6), (7) and (8) effectively represent the corona plasma discharge based on a first moment of the Bolzmann kinetic equation. Electron mobility, electron diffusion, collision ionization, attachment and recombination coefficients of the model are assumed to be a function of the locally reduced electric field E/N, where N is the neutral gas density and E is the local electric field. This indicates that relaxation times of the mean momentum and energy of the electron distribution is smaller than the timescales of the electric field variation. It is shown that the relaxation timescale of the electric field energy in the corona plasma layer is maintained on the magnitude of ps, while the typical timescale of the local field approximation in the corona plasma layer is usually measured in nanoseconds. This proves that the reduced electric field E/N is completely reasonable.

III. SOLUTION DOMAIN

The simplified AC line model may contain a number of infinite cylindrical conductors which parallel to each other above the ground level. A three-dimensional (3D) transmission line can follow a simplified transmission line model represented by a 2D model: equivalent to a line perpendicular to the plane.

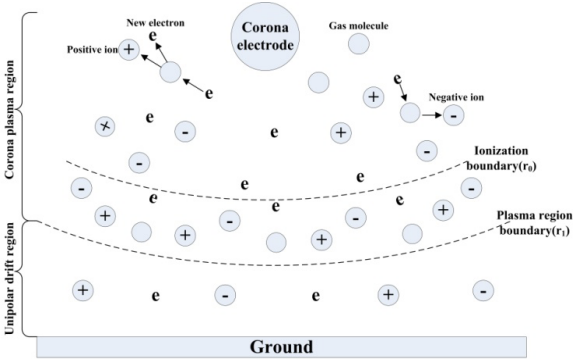

FIGURE 3. Model of an AC conductor corona discharge.

As shown in Figure 3, the domain of AC conductor corona discharge consists of a unipolar drift region and a corona plasma region. In a positive corona, the corona plasma region boundary is the ionization boundary. However, unlike the positive corona case, the negative corona plasma region boundary is extended from ionization boundary to the plasma region boundary, where the average kinetic energy of electrons is about 1.85 eV. The region between the ionization boundary and plasma region boundary is defined as corona-enhanced chemical reactions, where the electrons have enough energy to participate in the collision-reaction [9].

IV. NUMERICAL IMPLEMENTATION

With the variation of applied voltage, AC conductor has undergone non-corona, positive corona discharge and negative corona discharge, which have significantly different with the distribution of electrons and ions due to difference in generation and movement mechanisms. The following will be described separately.

A. POSITIVE HALF-CYCLE CORONA DISCHARGE

After the applied voltage becomes positive polarity, the electrons and negative ions formed in the last half-cycle will accelerate towards the conductor surface under the action of the electric field. At the initial stage of corona, the avalanche develops towards the conductor surface with the increasing electric field. The mobility of electrons is much greater than that of ions, so the electrons move rapidly towards the surface of the conductor, while the positive ions are left and move outward. When the avalanche reaches a certain number, the concentration of charged particles makes an obvious distortion to the external applied electric field. The streamer starts to form at this point which has a large amount of positive ions at the streamer plasma head and a weakly electric field in the plasma through which electrons are transferred to the conductor surface. Excited atoms (or molecules) produce a large number of photons during the de-excited process. In the air, these photons are mainly produced by the excited nitrogen molecules, $N_2\left(C^3\Pi_u\right)$ [22]. The radiated photons will cause photoionization, and the secondary electrons that sustain the discharge are generated in the gas phase by photoionization which occurs in the ionization layer. In the unipolar region, ionization and attachment are not considered ($\alpha = 0$, $\eta = 0$), while ion recombination before and after corona discharge includes respectively positive-ion-negative-ion recombination and electron-positive-ion.

Zheleznyak et al [23]–[25] proposed a photoionization model in the dry air, which is widely used. This model is based on the following two assumptions: First, the source of photoionization energy is the radiation of excited nitrogen molecules, $N_2\left(C^3\Pi_u\right)$; and second, the UV photons in the wavelength range 980-1025 Å are mostly absorbed by oxygen molecules and lead to photoionization. Under this premise, the nonlocal photoionization reaction depends on the gas composition and pressure. The photoionization rate at position $(\vec{r}_1, t)$ due to the absorption of the emitted photons from $(\vec{r}_2, t)$ is:

$$S_{ph}(\overrightarrow{r}_1, t) = \iiint \frac{I(\overrightarrow{r_2}, t) f(r)}{4\pi r^2} d\theta dr_1 dz_1 \tag{9}$$

where $r = \left|\overrightarrow{r_1} - \overrightarrow{r_2}\right|$ is a distance from $(\vec{r}_2, t)$ to $(\vec{r}_1, t)$; I is the number of photons released per unit time of the source volume and is assumed to proportional to the ionization production rate; the function $f(r)$ in the nitrogen-oxygen mixed gas is the portion of the radiation that is actually absorbed along the path r.

We assume that photoionization occurs only in the corona plasma layer, so the boundary of the photoionization model is selected as the ionization boundary. The photoionization at the boundary is calculated according to the Zheleznyak integral model (equation (9)).

TABLE 1. Boundary conditions for the positive corona discharge model.

Boundary conditions	Conductor surface	Ionization boundary	Artificial boundary	Ground
Electron	$-n\cdot D_e\nabla N_e=0$	$S_{ph}(r_o)$	$\begin{cases}-n\cdot D_e\nabla N_e=0 & \boldsymbol{\beta}_e(x)\cdot n(x)\geq 0\\ N_e=0 & \boldsymbol{\beta}_e(x)\cdot n(x)<0\end{cases}$	$-n\cdot D_e\nabla N_e=0$
Positive ion	$N_p=0$	$N_p(r_o)$	$\begin{cases}-n\cdot D_p\nabla N_p=0 & \boldsymbol{\beta}_p(x)\cdot n(x)\geq 0\\ N_p=0 & \boldsymbol{\beta}_p(x)\cdot n(x)<0\end{cases}$	$-n\cdot D_p\nabla N_p=0$
Negative ion	$-n\cdot D_n\nabla N_n=0$	$N_n(r_o)$	$\begin{cases}-n\cdot D_n\nabla N_n=0 & \boldsymbol{\beta}_n(x)\cdot n(x)\geq 0\\ N_n=0 & \boldsymbol{\beta}_n(x)\cdot n(x)<0\end{cases}$	$N_n=0$

The plasma kinetic model of positive half-cycle corona discharge is simulated by the equations (5)-(8), which include four variables to be solved: space potential, electron density, and positive and negative ion density. To solve these variables, the boundary conditions of the solution region must be set according to physical characteristics of the electron and ion in the corona plasma layer. In the light of the division of the solution boundary, the boundary conditions are as follows:

(1) For Poisson' equation, the conductor voltage and the ground potential are known. On the ionization boundary, where the reduced electric field E/N is 120Td (1Td $=10^{-21}\mathrm{Vm}^2$) and the ionization coefficient equate to the attachment coefficient.

$$\mathrm{E}(r_0)=3\times 10^6\ \mathrm{V/m} \tag{10}$$

(2) After the electrons reach the surface of the conductor, they are absorbed, so the flux appears as an outflow. When negative ions move toward the conductor surface, they are neutralized and disappear, so the flux is reflected as the outflow. Under the action of electric field, positive charge is far away from the conductor surface of the same polarity, so the positive ion density is set to zero at the conductor surface.

(3) The absorbing boundary condition [26] is applied to the outflow (upwind) part, that the outflow flux contribution in the edge integral along the absorbing boundary is eliminated.

(4) The negative ions at the ionization boundary consist of two parts: one is generated by the electron attachment and the other is the negative ions generated in the previous negative half-cycle drifting towards the ionization boundary under the influence of the electric field. Since the electron density and the attachment coefficient near the ionization boundary are very small, the first part can be neglected. The positive ions cross this boundary into the unipolar ion region; meanwhile, photoionization occurs at this boundary, where the electrons are produced.

The boundary conditions are summarized in Table 1, where $\boldsymbol{\beta}(x)$ is the space-charge drift velocity, $\boldsymbol{\beta}(x)=k\boldsymbol{E}$.

B. NEGATIVE HALF-CYCLE CORONA DISCHARGE

In the negative half-cycle corona, the high-energy electrons and positive ions near the negative conductor surface rapidly move to the lower field region. During their motion, they produce avalanches and leave low mobility positive ions in the space between them and the surface of the negative conductor. Therefore, plasma is formed in the vicinity of the surface of the negative conductor. The average kinetic energy of the ions in the corona plasma is about 0.01-0.1 eV, which is not sufficient to strike electrons from electrode. The short wavelength photons emitted in corona discharge have sufficient energy to ionize from the gas or to extract electrons from conductor surface. The ionization energy of oxygen and nitrogen is about 12.06 eV and 15.6 eV, respectively, while the electron removal from the conductor surface requires about 4 to 5 eV [2], which is significantly smaller than the former. Therefore, the most important mechanism for the generation of secondary electrons for negative corona discharge is the photoemission from conductor surface. With the continuous development of the secondary process, the field generated by the space charge causes a significant distortion of the external electric field. The field in the plasma is suppressed and the field at both ends is enhanced. Due to field suppression in the high field region and field enhancement only in the low field region, it is often found that the negative corona discharge is diffusive. Furthermore, the amount and energy of electrons become smaller and smaller with increasing distance from the conductor surface. Thus, the contribution of electrons to the reaction rate over a certain distance (corona plasma region) is negligible. Evans and Inculet (1978) found that the size of the negative corona visible region was thicker than that of the positive corona. Corona discharges of both polarities have the same size of the ionization region. However, for the negative corona discharge, the electrons have a sufficient amount and energy to cause the electron-impact reaction outside the ionization boundary. Therefore, the corona plasma region of the negative conductor is extended to the plasma boundary where the reduced electric field E/N is 80Td, unlike the positive corona where the corona plasma only extends to the ionization boundary. Outside the ionization boundary, attachment is dominant compared to ionization and the number of electrons decreases as the electric field decreases, hence only attachment is considered between the ionization boundary and plasma boundary. Consequently, the contribution of electrons to the reaction rate beyond a particular radial position is negligible. As electrons are far from the

TABLE 2. Boundary conditions for the negative corona discharge model.

Boundary conditions	Conductor surface	Plasma boundary	Artificial boundary	Ground
Electron	$N_e(D^s)$	$N_e(r_o)$	$\begin{cases} -n\cdot D_e\nabla N_e=0 & \boldsymbol{\beta}_e(x)\cdot n(x)\geq 0 \\ N_e=0 & \boldsymbol{\beta}_e(x)\cdot n(x)<0 \end{cases}$	$-n\cdot D_e\nabla N_e=0$
Positive ion	$-n\cdot D_p\nabla N_p=0$	$N_p(r_o)=0$	$\begin{cases} -n\cdot D_p\nabla N_p=0 & \boldsymbol{\beta}_p(x)\cdot n(x)\geq 0 \\ N_p=0 & \boldsymbol{\beta}_p(x)\cdot n(x)<0 \end{cases}$	$N_p=0$
Negative ion	$N_n=0$	$N_n(r_o)$	$\begin{cases} -n\cdot D_n\nabla N_n=0 & \boldsymbol{\beta}_n(x)\cdot n(x)\geq 0 \\ N_n=0 & \boldsymbol{\beta}_n(x)\cdot n(x)<0 \end{cases}$	$-n\cdot D_n\nabla N_n=0$

plasma boundary, their energy is significantly reduced, so that ionization and attachment are not considered in the unipolar region, whereas the recombination between ions remains.

Photoemission can occur in dielectric materials [2]. The photon energy threshold of photoemission depends on the bandgap, electron affinity and bulk polarization of the dielectric material. So far, the photoemission of metal electrode model has been established in [7]. On that basis, the photoemission physical model of the conductor surface in this paper is established by combining Beer-Lambert law and photoionization model. The electron density generated in the conductor surface unit D^s due to radiation from the element D^k can be approximated as:

$$N_e(D^s) = \frac{\gamma I(D^k) g(R)}{4\pi d^2} \tag{11}$$

here, γ is the photoemission coefficient, which depends on the cathode material, and is also very sensitive to the cathode surface conditions [7]; it generally varies from 0.001 to 0.01 (this paper takes 0.08). d is the distance between D^k and D^s. $I(D^k)$ is the number of photons released per unit time in D^k, in this model, to simplify the calculation, it is assumed that the production of photons is equal to the ionization production rate.

$$I(\mathrm{D}^k) = \alpha \cdot W_e(D^k) N_e(D^k) D^k dt \tag{12}$$

In the photoemission model, the photo radiation arising from gas discharge which produces photoemission is absorbed by ambient gas, which plays an important role. Assuming that the photoemission is carried out by the same high energy photons responsible for photoionization, the relationship between the absorption capacity of photos through the air and the depth of the absorbing medium follows Beer-Lambert Law [27].

$$g(R) = \int e^{-\mu d} cos\theta df \tag{13}$$

where θ is the angle between the radiation direction and the normal vector, and μ is the absorption coefficient. Oxygen and nitrogen predominate in the dry air, and N_2 is a radiation source. However, the absorption of radiation by the N_2 molecule at the relevant wavelengths is forbidden by quantum rules [25] and so it can be taken as negligible in the calculation. Therefore, in this paper the absorption coefficient of air is taken to be equivalent to that of oxygen. In the wavelength range of 98-102.5nm, the absorption coefficient of O_2 can be approximated as [28]:

$$\mu = \mu_1 (\mu_2/\mu_1)^{(f-f_1)/(f_2-f_1)} \tag{14}$$

where $\mu_1 = \xi_{\min} p_{O_2}$ and $\mu_2 = \xi_{\max} p_{O_2}$ are, respectively, the previously introduced oxygen minimum and maximum absorption coefficient. The frequency f range here corresponds to 98-102.5nm, which is considered a single state frequency unit range, and f_1 and f_2 are the minimum and maximum frequency value, respectively. Equation (14) is taken into equation (13) and integrated over the frequency range 98-102.5nm to give:

$$g(R) = \frac{(\mu_1 - \mu_2)(e^{-\mu_1 d} - e^{-\mu_2 d}) cos\theta}{d \ln(\mu_2/\mu_1)} \tag{15}$$

Since photoemission occurs only on the surface of the conductor, the electrons generated by the photoemission serve as boundary conditions for the model. Because of the nonlocality of the radiation, all the plasma in the computation domain must be included in the calculation of the radiation on the conductor surface. Furthermore, the computation domain is equivalent to two-dimensional. Therefore, photoemission is calculated using the same mesh as equations (5)-(8) in the photoemission calculation process.

The plasma kinetic model of negative half-cycle corona discharge is also simulated by the same equations (5)-(8) as the positive corona. However the physical process is completely different and hence the boundary conditions are now as follows according to the solution domain and the physical process and are summarized as shown in Table 2.

(1) On the artificial boundaries, the charged particles that arrive at this boundary are considered to leave the computational domain and disappear, and the flux will only appear as an outflow without inflow, and there is no charge source at the boundary. The reality of the artificial boundaries is approximated by a symmetry condition, and then zero gradient boundary condition is applied along the artificial boundaries [29]:

$$n \cdot (\varepsilon_0 \nabla u) = 0 \tag{16}$$

where n is the unit normal vector with respect to Γ.

(2) On the plasma boundary, the positive ions move towards the surface of the conductor under the action of a high electric field, so the positive ion is also negligible; however, negative ions, which are iteratively solved according to the known boundary electric field, enter the unipolar region through this boundary. At the ionization boundary, the attachment and ionization intensity are equal. When the electrons move beyond this boundary, the attachment begins to be greater than ionization, but the difference between the two is small. The number of electrons also slowly decreases as the electric field decreases. Therefore, based on the ionization and attachment processes in the ionization region, it is now assumed that the density of electrons at the ionization boundary is:

$$N_e(r_0) = \xi N_e(D^s) e^{\int_0^{r_0} (\alpha(r)-\eta(r))dr} \tag{17}$$

The variable ξ in equation (17) is assumed to be a fixed value according to the later numerical simulation of negative corona discharge. We have found that the position of the ionization boundary is slightly changed by appropriately adjusting variable ξ, but it does not change the discharge characteristics. It is found that the appropriate adjustment of this value has a slight effect on the location of the ionization boundary, but does not change the entire ion distribution.

(3) The secondary electrons emitted from the surface of the negative conductor do not have sufficient time to form negative ions in the vicinity of the surface of the conductor, so the density of negative ions is zero. Positive ions moving to the conductor surface are neutralized and disappear, so the positive ion flux appears to flow out on the conductor surface. The most important mechanism for the generation of secondary electrons of negative conductors is photoemission from the surface of the discharge electrode so that the electron density on the surface of the negative conductor is calculated according to the photoemission.

(4) When the electrons and negative ions arrive at the ground, they disappeared and the flux will only show the outflow, no inflow.

C. WITHOUT CORONA DISCHARGE MODEL

As shown in Figure 1, the space charge before the corona is neglected in the first cycle of power-up, but then when the voltage is again below the onset voltage, the charge distribution still follows the hydrodynamics convection-diffusion model (the equations (5)-(8)) due to the presence of a large amount of space charge around the conductor. The whole calculation area includes only the unipolar region, and its calculation is still in accord with the above described unipolar mathematical model. However, since space charge accumulates in the corona stage, ion recombination still exists. At this time, the space charge distribution calculated from the corona at the previous time is taken as its initial condition (including the conductor surface). The boundary includes the conductor surface, the ground and the artificial boundary. Furthermore, the electric field on the conductor surface is calculated using the EPRI empirical formula [30] since there is no corona discharge.

$$E_{surface} = \frac{U}{r\ln(2H/r)} \tag{18}$$

where U, r and H is the applied voltage, conductor radius and the height of the conductor above ground, respectively.

D. CORONA CURRENT

Under the influence of periodically reversing electric field, the space charges generated by corona discharge on the AC conductor surface are constrained to make a reciprocating motion within the vicinity of the conductor. The current to the conductor induced by charge motion is determined by [31], [32].

$$I_i = q_i E_v v \tag{19}$$

where E_v is the nominal electric field at the location of the moving charge when the space charge is removed and the conductor is applied to unit potential (v-direction electric field component). v is the ion velocity, and q_i is the charge quantity.

The corona current is the induced current of space charges generated by corona discharge on the conductor surface. The current produced by the displacement charge contains additional corona capacitor current I_{cap} and corona current [30]. The induced current in the conductor by any given motion of space charge is calculated by equation (19), and these induced currents are summed to obtain the corona current of the conductor.

$$\begin{aligned} I &= I^+ - I^- - I_{cap} \\ &= \sum_{n=1}^{N} (\rho_n^p S_n E_{vn} v_n^+ - (\rho_n^n + \rho_n^e) S_n E_{vn} v_n^-) - \frac{d\sum_M q_{cond}}{dt} \end{aligned} \tag{20}$$

here, S_n is the area of the mesh where the node is located. q_{cond} is the amount of conductor simulation charge in the absence of space charge, which is solved by the known potential coefficient and the Maxwell potential coefficient matrix under the condition of absent space charges [15].

V. RESULT

The corona current and ion distribution of positive and negative half-cycles of corona discharge of AC conductor in dry air are numerically simulated by using the physical model proposed in this paper. The scheme that adopts Discontinuous Galerkin Time-Domain (DGTD) Method numerical calculations to study each physical quantity is followed.

A. CORONA CURRENT

For the single-phase AC conductor (the radius is 0.9cm) arrangement in a cylindrical experimental cage (the radius is 26cm), the corona current simulation and measurement results are shown in Figure 4, where simulation curve is

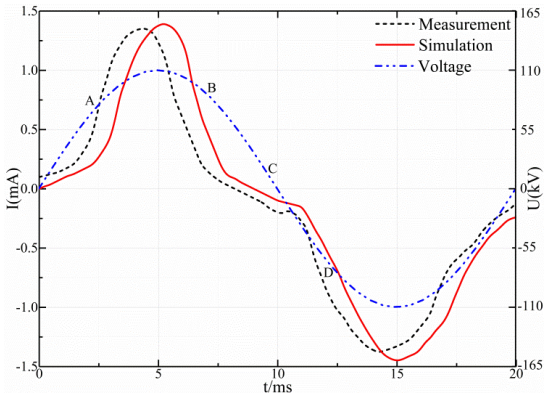

FIGURE 4. Corona current waveform.

the result calculated from the AC corona discharge physics model presented in this paper, and measurement curve is the measurement result of [30].

The corona current determined by simulation shows a phase lag compared to the measured current (see Figure 4). The reason for this is that the roughness factor of the measured conductor is different from that set out in this paper and the onset field of the latter is smaller than the former. Furthermore, it should be noted that the simulation curve starts from the zero, which is different from measurement curve. This can be explained that the ambient seed electrons around the conductor induce a certain electric field near the conductor, thus forming an induced current before the applied voltage on conductor. However, the corona current waveform calculated by using the physical model proposed in this paper is basically consistent with the development trend of the measured current waveform. Thus, the effectiveness of the method proposed in this paper is verified. By comparing Figures 4 and 1, it is found that the corona current is ahead of the voltage in phase. Before the conductor voltage reaches corona onset field (before point A in Figure 1), the seed electrons accelerate closer to the conductor and the induced current slowly increases since there is no new generation of charged particles with the increases of applied voltage. After corona discharge, a large number of electrons, and positive and negative ions are generated by corona discharge to maintain the corona current. When the conductor voltage is peaked and then falls below the corona onset field (point B in Figure 1), the ions in the space rapidly reduce and move away from the conductor. Thus, the corona capacitor current becomes the dominant charge current under the action of the electric field. The corona current has been reversed to negative polarity when the corona is stopped but the voltage is still positive (after point C in Figure 1). After the voltage enters the negative half-cycle, the corona current generated by the movement of space charges produced in the positive half-cycle increases slowly since these space charges are relatively distant from conductor surface and in a small electric field. After the negative corona discharge (point D in Figure 1) is reached, the corona current starts to increase, and then the subsequent process is similar to the positive half-cycle.

B. POSITIVE HALF-CYCLE CORONA DISCHARGE

In this paper, the positive and negative half-cycle corona discharge process of a single-phase AC conductor with radius and height of 0.1mm and 80cm is numerically simulated. The applied single-phase AC voltage is 40kVrms, which is higher than the corona onset voltage. The electric field distribution at different moments is shown in Figure 5.

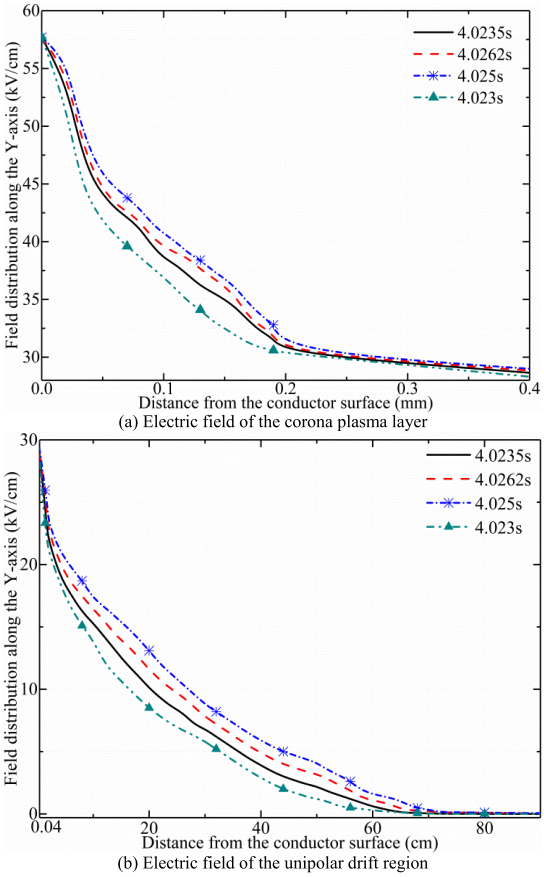

FIGURE 5. Field distribution along the y-axis at different moments.

As shown in Figure 5, the electric field of the whole single-phase AC conductor consists of two parts: the electric field of the corona plasma layer and the unipolar electric field, and which are 3.0×10^6V/m as the demarcation point of the electric field. Since the conductor voltage after the peak begins to reduce, and while the external electric field gradually reduces, a large number of positive charges accumulated in the streamer head diminish the electric field of the plasma region. Consequently, the electric field of the curve 4.0262s in the middle of the corona plasma layer where the streamer begins to form is smaller than the curve 4.0235s. In the unipolar region, the ionization process is not considered due to the sharp decline in the electric field, and the recombination between the ions is relatively weak, so that the electric field decreases relatively slowly as the distance increases.

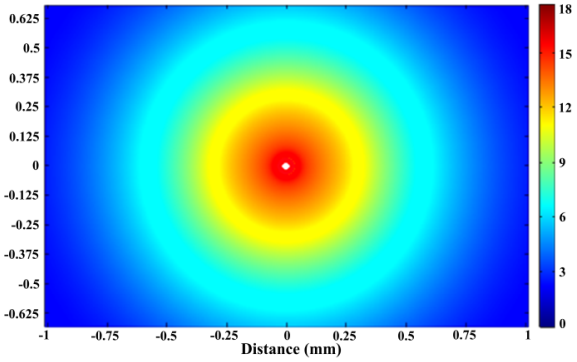

FIGURE 6. Electron distribution at time of 4.025s (contour plots in log10 scale).

Figure 6 shows the 2D distribution of electron density at time of 4.025s. In the corona plasma layer, the only source of secondary electrons is photoionization, which means that the next avalanche will occur immediately when the last time the avalanche is absorbed at the positive conductor surface. The sufficient supply of electrons in the corona plasma layer will provide a stable electron for the streamer propagation, so that the streamer branching does not exist. In the corona plasma layer, with the passage of time, the distribution of charged particles has undergone an obvious change, as shown in Figure 7. This is mainly reflected in the changes with the electric field and the boundary of the corona plasma region is basically maintained at 0.29mm from the conductor surface. As the electric field increases, the distribution of charged particles, the ionization and attachment intensity, and the positive, negative ions mobility are increasing. Consequently the positive ion density increases rapidly from zero at the conductor surface and then increases slowly. The area where the streamer extends outward gradually becomes larger. Since the close proximity to the ionization boundary, the intensity of attachment and ionization is getting closer and closer, so that adjacent time-steps are very close when the electron density approaches the ionization boundary. At the same time, since the reduction in magnitude of the electric field has significantly slowed down nears the ionization boundary, as shown in Figure 5, the negative ions near the ionization boundary show very close at the adjacent time. In the unipolar region, the ionization process is not considered, and the recombination between ions is relatively weak, so that the ion density increases relatively slowly as the increase of the applied voltage.

C. NEGATIVE HALF-CYCLE CORONA DISCHARGE

The reduced electric field of plasma layer boundary is 80Td (about 2.0×10^6V/m). As shown in Figure 1, the time of the point B to point C of the positive half-cycle of the applied voltage is approximately 4ms, and the positive ions mobility is on the order of 10^{-4}. Thus, according to the ion drift velocity kE, there is still a positive ion between the conductor surface and the ground when the voltage reaches point C.

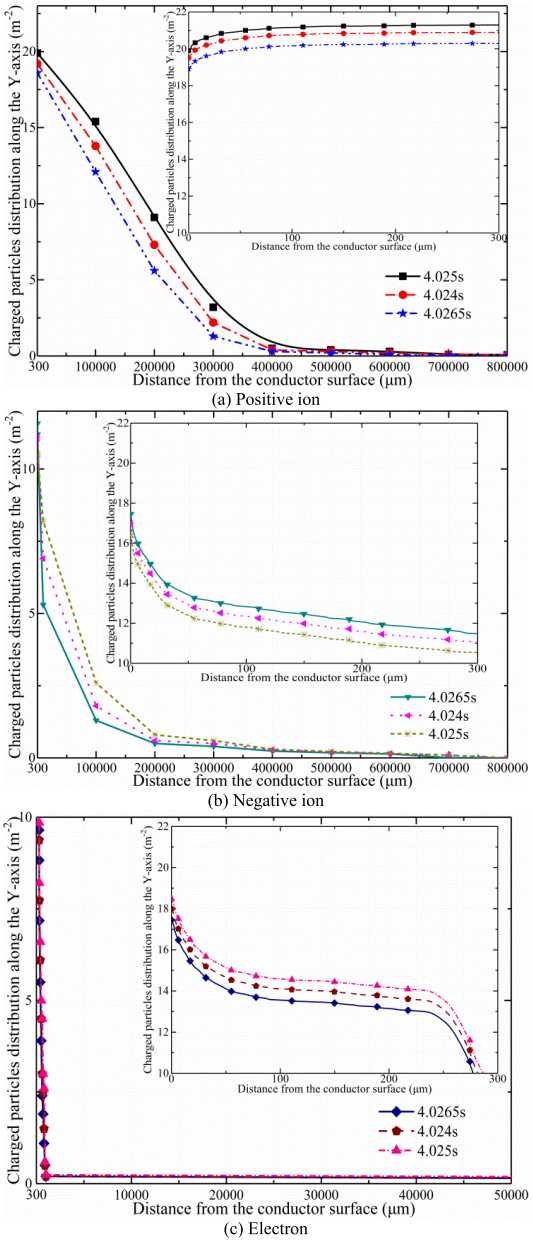

FIGURE 7. The charged particle distribution of the positive half-cycle along the y-axis at critical times (the ordinate is in log10 scale).

Therefore, the effect of the positive ions produced in the positive half-cycle must be taken into account in calculating the distribution of charged particles in the negative half cycle. From point C to point D in Figure 1, since no corona occurs at this stage, the ion distribution is calculated in terms of space only positive charge of the unipolar mode. From point D to point E in Figure 1, the effect of the positive ion generated in the positive half cycle must be considered.

In the corona plasma region, the distribution of electron, negative ions and positive ion density is completely different, as shown in Figure 8. The electron density begins to increase from the surface of the conductor and begins to decrease as it approaches the plasma boundary. The electrons at the

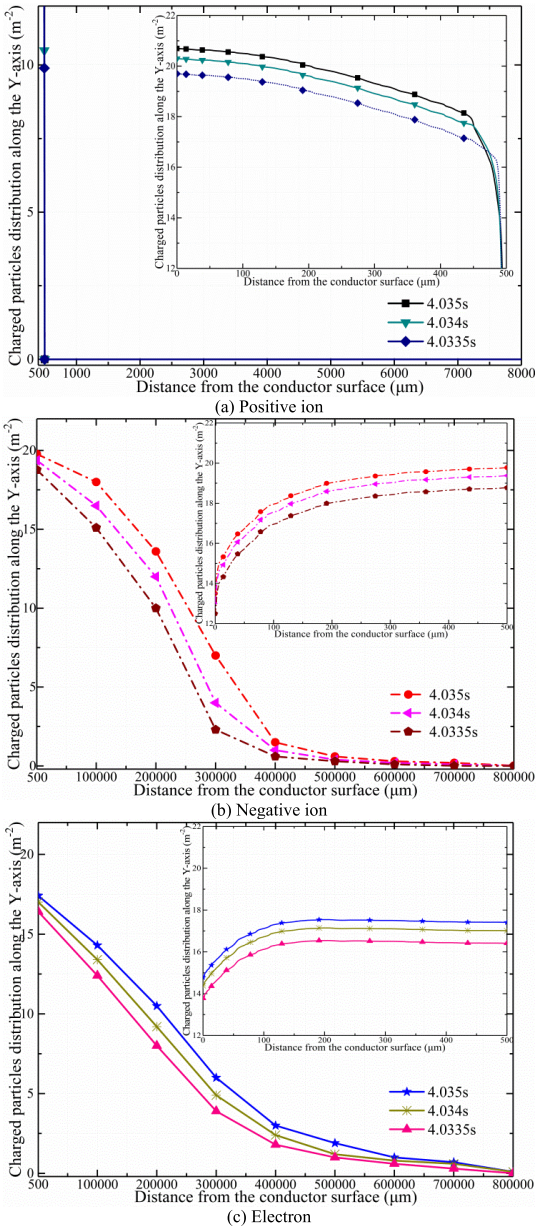

FIGURE 8. **The charged particle distribution of the negative half-cycle along the y-axis at critical times (the ordinate is in log10 scale).**

conductor surface are electrons required to maintain their self-sustaining discharge by photoemission on the surface of the negative conductor. Subsequently, these electrons are ionized with the gas molecules under the action of the electric field and the electron density begins to increase. The electron density begins to decrease as the electric field intensity decreases sharply near the corona layer boundary. The density of the negative ions increases from zero at the surface of the conductor to the maximum at the outer edge of the plasma, where it is considerably higher than the electron density. While the density of positive ions is the largest at the surface of the conductor and then slowly decreases with increasing distance from the conductor surface, but eventually becomes zero when approaching the plasma boundary. The distribution of positive ions is completely different from that of electrons and negative ions, which can be explained that the ionization process is dominated over the attachment in the corona layer, and meanwhile the positive ions move quickly toward the surface of the negative conductor under the action of the electric field.

Figure 8 shows the distribution of charged particles at different moments of the negative half-cycle of the AC voltage. As can be seen from Figure 8, the thickness of the corona layer at different times of the negative half cycle of the AC voltage after the corona is substantially the same. This phenomenon can be explained that the surface electric field of the conductor meets the Peek's onset field after the corona discharge; that is, the electric field strength of the conductor surface after the conductor corona is assumed to be equal to the value given by Peek's empirical formula, which does not change with the vary of the conductor voltage, but the distribution of the charged particles changes with the change of the applied voltage. As shown in Figure 8, the corresponding applied voltage (the applied voltage in Figure 8 at different moments is calculated according to the equation (2)) continues to increase over time, and more space charge will accumulate in the corona layer and the unipolar region, so that the density of space charge is increasing. Therefore, when approaching the boundary of the plasma layer, the rapid descent zone of the positive ion density is slowly advanced. This means that a stronger charge flux generates a stronger streamer, which resulting in a stronger electric field on the conductor surface. In the unipolar layer, since the velocity of electron transport is significantly larger (two orders) than that of negative ions, the negative ion density curve decreases rapidly over 30 cm from the conductor surface, which is lower than the electron density.

D. COMPARISON OF POSITIVE AND NEGATIVE HALF-CYCLE CORONA DISCHARGE PROCESS

According to the above analysis, the plasma generation and motion mechanisms in the positive and negative half-cycle corona discharges are completely different, and the comparison between the two is shown in Figure 9. In the corona plasma region, the total number of electrons generated by the negative half-cycle corona is much larger than the total number of electrons generated by the positive half-cycle corona. The reason is that the electrons generated by the positive half-cycle corona will be continuously neutralized by the conductor surface, and the number of electrons generated by the photoemission is greater than that of the photoionization. However, the number of high-energy electrons in the higher electric field near the conductor surface is more in the positive discharge, so that the effect of the discharge polarity on the electron-collision reaction rate depends on the energy threshold of the reaction. With the increase of the distance from the conductor surface, the number of negative ions in the negative half-cycle continues to increase and reaches the maximum at the ionization boundary. In the positive half-cycle, the negative ions are continuously decreasing and become zero when

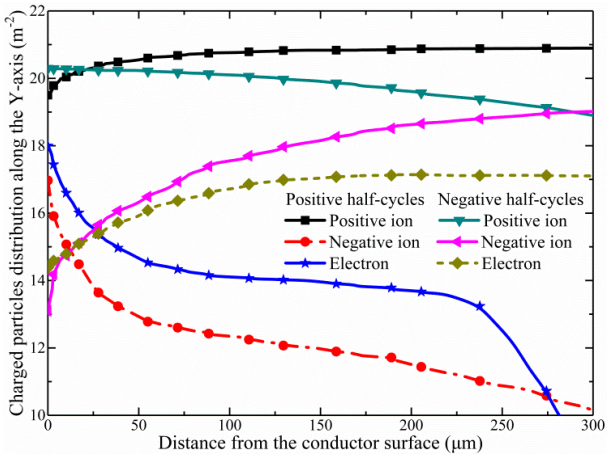

FIGURE 9. Comparison of charged particle distribution of positive and negative half-cycle (the ordinate is in log10 scale).

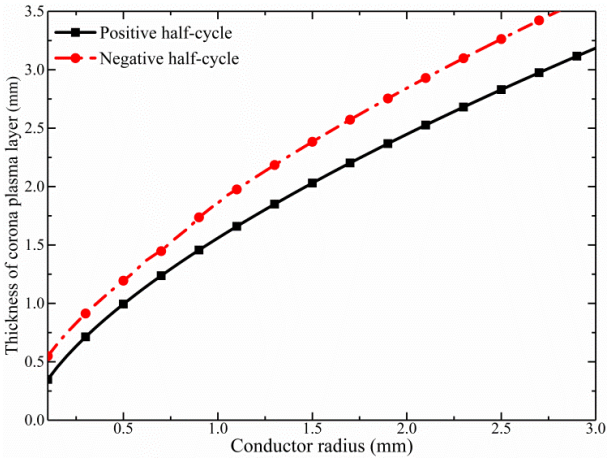

FIGURE 10. The thickness of positive and negative half-cycle corona plasma layer varies with the conductor size.

approaching the ionization boundary. Because ionization is better than attachment, the number of positive ions generated by positive and negative half-cycle corona in the ionization area is not much different, and it gradually increases as it gradually moves away from the conductor surface.

The applied voltage has little effect on the thickness of the corona plasma region [9]. In the corona plasma region, since the number of electrons generated in the negative half-cycle corona discharge is much larger than that in the positive half-cycle corona discharge. In addition, the electrons of negative half-cycle have more energy at the ionization boundary. Finally, the plasma region of the negative corona discharge as shown in Figure 10 is larger than that of the positive corona discharge.

VI. CONCLUSION

The complex micro-physical processes of corona discharge of single-phase AC line at atmospheric pressure in dry air are studied in this paper. These studies enable us to obtain valuable insight into the effects of avalanche and streamer in the corona layer on the expansion and propagation of the large space corona discharge and those microscopic parameters, such as plasma and field distributions, which are very difficult to study experimentally.

The photoionization and photoemission of the self-sustaining discharge in the corona layer produces a sufficient amount of electrons which supply streamer development so that streamer branching does not occur. The thickness of the corona layer does not change with the variation of applied voltage after corona of the single-phase AC conductor, but the distribution of the plasma in the corona layer changes significantly as the applied voltage changes.

The plasma in the period of AC voltage is confined in a very small space of about 0.29mm. The thickness of the corona plasma region remains essentially constant over the entire cycle, and the negative half cycle-of the corona plasma region increases the region between the ionization boundary and the ion boundary compared to the positive half-cycle.

In the positive half-cycle, the density of the positive ions in the corona layer is significantly larger than the density of the negative ions and electrons. The density peak of the electrons is greater than that of negative ions. In the negative half-cycle, the electron density starts to increase from the conductor surface and begins to decrease near the plasma boundary. The density of the negative ions increases from zero at the conductor surface to the maximum at the plasma boundary, where it is much higher than the electron density. The density of the positive ions is the largest at the conductor surface, and then slowly decreases. These changes have been demonstrated as a consequence of the difference in the primary and secondary processes of the positive and negative corona discharge.

The simulation does not yet account for the corona discharge process of the multiphase AC line. In the power system, the distance between the multi-phase lines of the AC transmission line is large, and the charge generated by other phases has little effect. Therefore, the influence of multi-phase voltage on corona discharge characteristics can be ignored.

ACKNOWLEDGMENT

The authors would like to thank Dr L. A. Dissado for his fruitful discussion and the English corrections of this paper.

REFERENCES

[1] F. W. Peek, *Dielectric Phenomena in High-Voltage Engineering*. New York, NY, USA: McGraw-Hill, 1929.
[2] Y. P. Raizer, *Gas Discharge Physics*. New York, NY, USA: Springer-Verlag, 1991.
[3] G. W. Penney and G. T. Hummert, "Photoionization measurements in air, oxygen, and nitrogen," *J. Appl. Phys.*, vol. 41, no. 2, pp. 572–577, Feb. 1970.
[4] S. Pancheshnyi, "Role of electronegative gas admixtures in streamer start, propagation and branching phenomena," *Plasma Sour. Sci. Technol.*, vol. 14, no. 4, pp. 645–653, Nov. 2005.
[5] Y. Zhang, Y. Han, W. Zheng, J. Yang, L. Qu, G. Liu, X. Zhao, and L. Li, "Study on spatial-temporal distribution characteristics of the discharge process in a 1 m rod-plate gap under different polarity lightning impulses," *IEEE Access*, vol. 7, pp. 111396–111410, 2019.

[6] A. A. Kulikovsky, "The role of the absorption length of photoionizing radiation in streamer dynamics in weak fields: A characteristic scale of ionization domain," *J. Phys. D, Appl. Phys.*, vol. 33, no. 1, pp. L5–L7, Jan. 2000.
[7] G. E. Georghiou, R. Morrow, and A. C. Metaxas, "The effect of photoemission on the streamer development and propagation in short uniform gaps," *J. Phys. D, Appl. Phys.*, vol. 34, no. 2, pp. 200–208, Jan. 2001.
[8] A. Hallac, G. E. Georghiou, and A. C. Metaxas, "Secondary emission effects on streamer branching in transient non-uniform short-gap discharges," *J. Phys. D, Appl. Phys.*, vol. 36, no. 20, pp. 2498–2509, Oct. 2003.
[9] J. Chen and J. H. Davidson, "Model of the negative DC corona plasma: Comparison to the positive DC corona plasma," *Plasma Chem. Plasma Process.*, vol. 23, no. 1, pp. 83–102, Mar. 2003.
[10] Y. V. Serdyuk, A. Larsson, S. M. Gubanski, and M. Akyuz, "The propagation of positive streamers in a weak and uniform background electric field," *J. Phys. D, Appl. Phys.*, vol. 34, no. 4, pp. 614–623, Feb. 2001.
[11] S. K. Dhali and P. F. Williams, "Two-dimensional studies of streamers in gases," *J. Appl. Phys.*, vol. 62, no. 12, pp. 707–4696, 1987.
[12] P. A. Vitello, B. M. Penetrante, and J. N. Bardsley, "Simulation of negative-streamer dynamics in nitrogen," *Phys. Rev. E, Stat. Phys. Plasmas Fluids Relat. Interdiscip. Top.*, vol. 49, no. 6, pp. 5574–5598, Jun. 1994.
[13] Y. Kang, G. Wu, X. Zhang, Y. Guo, C. Shi, and Y. Liu, "Polarity effect of flowing air discharge," *IEEE Access*, vol. 6, pp. 61819–61825, 2018.
[14] Y. Tian, X. Huang, W. Tian, Y. Zhu, L. Zhao, and Y. Zhang, "Study on the hybrid ion-flow field of HVDC and HVAC transmission lines by the nodal discontinuous Galerkin time-domain method," *IET Gener., Transmiss. Distrib.*, vol. 11, no. 1, pp. 209–217, Jan. 2017.
[15] M. Abdel-Salam and E. Z. Abdel-Aziz, "A charge simulation based method for calculating corona loss on AC power transmission lines," *J. Phys. D, Appl. Phys.*, vol. 27, no. 12, pp. 2570–2579, Dec. 1994.
[16] U. Straumann, "Simulation of the space charge near coronating conductors of AC overhead transmission lines," *J. Phys. D, Appl. Phys.*, vol. 44, no. 7, Feb. 2011, Art. no. 075502.
[17] T. N. Tran, I. O. Golosnoy, P. L. Lewin, and G. E. Georghiou, "Numerical modelling of negative discharges in air with experimental validation," *J. Phys. D, Appl. Phys.*, vol. 44, no. 1, Jan. 2011, Art. no. 015203.
[18] N. Liu, "Effects of photoionization on propagation and branching of positive and negative streamers in sprites," *J. Geophys. Res.*, vol. 109, no. A4, 2004, Art. no. A04301.
[19] R. Morrow and T. R. Blackburn, "The role of photoionization in streamer discharge formation in voids," *IEEE Trans. Plasma Sci.*, vol. 27, no. 1, pp. 26–27, 1999.
[20] I. Odrobina and M. Cernak, "Numerical simulation of streamer–cathode interaction," *J. Appl. Phys.*, vol. 78, no. 6, pp. 3635–3642, 1995.
[21] R. Morrow and J. J. Lowke, "Streamer propagation in air," *J. Phys. D, Appl. Phys.*, vol. 30, no. 4, pp. 614–627, 1997.
[22] J. Dutton, "A survey of electron swarm data," *J. Phys. Chem. Reference Data*, vol. 4, no. 3, pp. 577–856, Jul. 1975.
[23] M. B. Zheleznyak, A. K. Mnatsakarian, and S. V. Sizyk, "Photoionisation of nitrogen and oxygen mixtures by radiation from gas discharges," *Teplofizika Vysokikh Temperatur.*, vol. 20, no. 3, pp. 423–428, 1982.
[24] A. Luque, U. Ebert, C. Montijn, and W. Hundsdorfer, "Photoionization in negative streamers: Fast computations and two propagation modes," *Appl. Phys. Lett.*, vol. 90, no. 8, Feb. 2007, Art. no. 081501.
[25] A. Bourdon, V. P. Pasko, N. Y. Liu, S. Célestin, P. Ségur, and E. Marode, "Efficient models for photoionization produced by non-thermal gas discharges in air based on radiative transfer and the helmholtz equations," *Plasma Sour. Sci. Technol.*, vol. 16, no. 3, pp. 656–678, Aug. 2007.
[26] T. Colonius, "Modeling artificial boundary conditions for compressible flow," *Annu. Rev. Fluid Mech.*, vol. 36, pp. 315–345, Jan. 2004.
[27] K. Fuwa and B. L. Valle, "The physical basis of analytical atomic absorption Spectrometry. The pertinence of the beer-lambert Law.," *Anal. Chem.*, vol. 35, no. 8, pp. 942–946, Jul. 1963.
[28] A. K. Mnatsakanyan and G. V. Naidis, "Charged particle production and loss processes in nitrogen-oxygen plasmas," *Rev. Plasma Chem.*, vol. 1, pp. 259–292, Jan. 1991.
[29] T. Farouk, B. Farouk, D. Staack, A. Gutsol, and A. Fridman, "Simulation of DC atmospheric pressure argon micro glow-discharge," *Plasma Sour. Sci. Technol.*, vol. 15, no. 4, pp. 676–688, Nov. 2006.
[30] J. G. Anderson, "Lightning performance of transmission lines," in *Transmission Line Reference Book 345 kV and Above*. New York, NY, USA: EPRI, 1980.
[31] W. Shockley, "Currents to conductors induced by a moving point charge," *J. Appl. Phys.*, vol. 9, no. 10, pp. 635–636, Oct. 1938.
[32] S. Ramo, "Currents induced by electron motion," *Proc. IRE*, vol. 27, no. 9, pp. 584–585, Sep. 1939.

YI TIAN received the Ph.D. degree in electrical and mechanical engineering from Xidian University, Xi'an, in 2017. He is currently a Lecturer with the Department of Electrical Engineering, Xi'an Polytechnic University. His research interests include condition monitoring, fault diagnosis, and insulation life-span evaluation for electrical equipment.

CHIFENG LIU, photograph and biography not available at the time of publication.

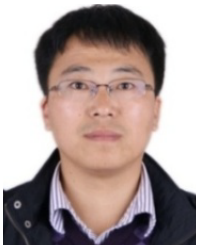

XINBO HUANG (Senior Member, IEEE) received the Ph.D. degree in automation from Xidian University, Xi'an, China, in 2005. Since July 2005, he has been a Teacher with Xi'an Polytechnic University, and since December 2008, he has been a Full Professor with the School of Electronics Information, Xi'an Polytechnic University. From 2005 to 2008, he held a postdoctoral position at the State Key Laboratory of Electrical Insulation and Power Equipment and the School of Electrical Engineering at Xi'an Jiaotong University, engaged in the snow and ice warning system on transmission lines. Since 2009, he holds postdoctoral position at the South China University of Technology, engaged in the transmission conductor galloping monitoring and mechanism. His current research interests include condition monitoring, fault diagnosis, and insulation life-span evaluation for electrical equipment.

WENCHAO TIAN received the Ph.D. degree in mechanical design and manufacture and automation from Xidian University, Xi'an, in 2004. He is currently a Professor with the School of Electro-Mechanical Engineering, Xidian University. He has over 80 publications on the MEMS and electro-mechanics. His research interests are MEMS, fluid dynamic, and electronic packaging.

WEN CAO, photograph and biography not available at the time of publication.

YONGCAN ZHU, photograph and biography not available at the time of publication.

LONG ZHAO, photograph and biography not available at the time of publication.